Contents lists available at ScienceDirect

Nuclear Instruments and Methods in Physics Research B

BEAM INTERACTIONS WITH MATERIALS AND ATOMS

CrossMark
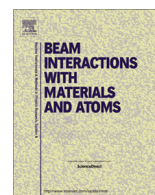
Swift heavy ion induced nano-dimensional phase separation in liquid immiscible binary Mn–Bi

S.K. Srivastava [a,*], S.A. Khan [b], P. Sudheer Babu [c], D.K. Avasthi [b]

[a] Department of Physics and Meteorology, Indian Institute of Technology, Kharagpur 721302, India
[b] Inter University Accelerator Centre, Aruna Asaf Ali Marg, P.O. Box 10502, New Delhi 110067, India
[c] Department of Physics, RGUKT, Nuzvid 521201, India

ARTICLE INFO

ABSTRACT

Pulsed laser deposited 60 nm thin film of homogeneous $Mn_{0.82}Bi_{0.18}$ composite has been irradiated by 100 MeV Au ions at fluence 1×10^{13} ions/cm^2, and investigated by field emission scanning electron microscopy, X-ray diffraction, magnetic hysteresis, X-ray photoelectron spectroscopy, and nanoindentation measurements. Dispersed nanostructures of soft Bi-rich phase of about 20 nm diameter emerged in a hard Mn-rich matrix on irradiation. Such structures, as synthesized by the present novel swift heavy ion irradiation approach, are usable as self-lubricating thin films.

© 2014 Elsevier B.V. All rights reserved.

1. Introduction

Materials composed of dispersed soft metal nanoparticles in hard metal matrix have potential applications as solid lubricants in advanced bearing systems [1,2]. Attempts are made to synthesize such structures by rapid thermal annealing of liquid immiscible binaries at earth [3,4] and in space [5,6], but the density difference induced stratification and Marangoni motion lead to stratification and coarse phase separation. In this context, a different materials synthesis technique, viz., ion beam processing, is worth viewing upon. Swift heavy ions (SHI's), which have immense potential of liquefying metals in nanosized latent tracks and cool them extremely rapidly at a rate of about 10^{14} K/s [7,8], could be a very suitable means to synthesize such phase-separated nanostructures. Precipitation of C nanoclusters in ion-irradiated polymers and gels [9,10], Fe and Co nanoparticles in polymers [11], and noble metal nanoparticles embedded in oxide matrices [12] are some reports of nanophase formation using ion beams. As far as studies on liquid immiscible elements are concerned, there are reports only on the ion irradiation of multilayers: (i) by Enrique et al. [13], who report a semi-coherent decomposition of nanostructures on 1 MeV Kr, 125 °C irradiation of Ag/Cu multilayer, and (ii) by Gao et al. [14], who observed an irradiation resistance and immiscibility in W/Cu multilayers.

The Mn–Bi phase diagram possesses a liquid miscibility gap in 55–100 atomic percent Mn, and 1235–1800 °C temperature,

ranges [15]. A homogeneous mixture of Mn and Bi with Mn as the majority component is expectedly highly susceptible to the mechanism described by the thermal spike model [8] because of the high e–p coupling – about 10^3 W cm^{-3} K^{-1} in Mn as opposed to 125 W cm^{-3} K^{-1} for Fe [7], for which lattice temperatures are reported in [8]. Thus, SHI irradiation of homogeneous Mn–Bi composite thin film has a potential to generate structures with soft, possibly Bi, nanoparticles dispersed in hard, possibly Mn, matrix.

In the present work, we synthesize a thin-film structure with soft Bi nanoparticles dispersed in a hard Mn-rich matrix by 100 MeV Au ion irradiation of a homogeneous $Mn_{0.82}Bi_{0.18}$ composite thin film.

2. Experimental

Appropriate amounts of $\sim$99.99% pure metallic Mn and Bi from Alfa Aesar were first melted together in an argon arc furnace and cooled to form a solid composite, which was then crushed and pelletized. A thin film was deposited on a quartz substrate from this pellet by pulsed laser deposition. The composition $Mn_{0.82}Bi_{0.18}$ of the film was determined by energy dispersive X-ray spectroscopy. The film was then cut into two parts, one of which was irradiated by 100 MeV Au ions at 1×10^{13} ions/cm^2 fluence using the 15 UD Pelletron accelerator at IUAC, New Delhi. The electronic and nuclear energy losses, S_e and S_n, respectively, of the ion in the composite, as calculated using TRIM [16], are $\sim$22.8 keV/nm and $\sim$0.6 keV/nm, respectively, suggesting the dominance of S_e and applicability of the thermal spike model. The samples were characterized by field emission scanning electron microscopy (FESEM), X-ray diffraction

* Corresponding author. Tel.: +91 3222 283854, mobile: +91 9735444091.
E-mail address: sanjeev@phy.iitkgp.ernet.in (S.K. Srivastava).

(XRD), X-ray reflectivity (XRR), magnetization, X-ray photoelectron spectroscopy (XPS) and nanoindentation measurements. FESEM was performed using Carl Zeiss SUPRA 40 Field Emission Scanning Electron Microscope, the XRD, using Philips X'Pert diffractometer with Cu K$_\alpha$ radiation, the XRR, in the P08 beamline of PETRA III, DESY, Hamburg, Germany, the magnetization versus magnetic field, using Quantam Design SQUID magnetometer, the XPS, using PHI VersaProbeII system, and the nanoindentation using Hysitron TriboIndenter.

3. Results and discussion

3.1. Field emission scanning electron microscopy

The FESEM images of the pristine and irradiated samples are shown in Fig. 1. The pristine sample displays homogeneity in the surface morphology indicating that Bi and Mn are in a mixed state on deposition. After irradiation, the surface morphology features brighter nanostructures of ~20 nm sizes and presumably of Bi-rich phase dispersed in a matrix of darker, presumably Mn-rich, phase. This observation is an evidence of nanophase separation induced in $Mn_{0.82}Bi_{0.18}$ film by the SHI.

3.2. X-ray diffraction and X-ray reflectivity

The XRD patterns of the pristine and irradiated samples are shown in Fig. 2. The pattern for the pristine sample is quite featureless, except for one small peak corresponding to Mn (1 1 2) [17]. This peak in fact occurs at an angle 0.14° greater than the pure Mn value, indicating that Mn is embedded with atoms of Bi, which has smaller lattice constant than that of Mn, an observation in consistence with the FESEM picture. Traces of Bi (2 0 2) and MnO_2 (1 1 1) peaks can also be identified, but they are very broad and of low intensity. It means Bi is not in its crystalline form; rather Bi atoms are homogeneously distributed in Mn matrix. The minor oxidation of Mn is insignificant. On irradiation, the above peaks get enhanced and a new shifted Mn (2 1 1) peak emerges, indicating a separation of Mn-rich and Bi phases. The thickness of the film was determined to be 60 nm by XRR. The inset of Fig. 2 shows the XRR curve and its fit using PARRATT32 code for the pristine sample as a representative data.

3.3. Magnetic hysteresis

Fig. 3 shows the magnetic hysteresis curves for pristine and irradiated samples at 10 K (Fig. 3a) and at 300 K (Fig. 3b). The linear component of the curve, arising collectively from possible and unresolvable paramagnetism of Mn and diamagnetism of Bi and substrate, has been subtracted from the curves. At both the
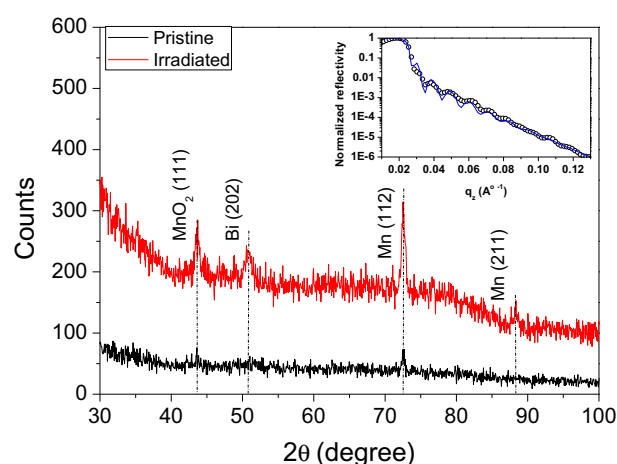

Fig. 2. XRD patterns of pristine and irradiated samples. Inset: XRR curve and its fit for the pristine sample.

temperatures, the pristine sample exhibits a hysteresis loop, the area of the loop being larger at the lower temperature. This temperature dependence of the hysteresis loop area is indicative of presence of ferromagnetism in the pristine sample. Pure Mn is known to be paramagnetic [18], while Mn with Bi, as in BiMn phase [19], is ferromagnetic. Thus, it can be inferred that the pristine sample is a composite of Mn and Bi, as evidenced also by FESEM and XRD. On irradiation, there is a further reduction in the coercivity as well as in the saturation magnetization at both temperatures. This is indicative of a loss of ferromagnetism and appearance of paramagnetism due to separation of Mn from Mn–Bi composite on irradiation, an inference also obtained from the FESEM and XRD results.

3.4. X-ray photoelectron spectroscopy

Fig. 4 displays the XPS spectra for pristine and irradiated samples in Mn 2p, O 1s and Bi 4f regions. The Bi $4f_{7/2}$ peak for the pristine sample occurs at 158.1 eV, while the elemental Bi peak occurs at 157.0 eV [20]. This peak must arise due to Mn neighborhood around Bi atoms, indicating a mixture of Bi and Mn. The Mn $2p_{3/2}$ peak at 639.9 eV is also correspondingly higher than the pure Mn value [21]. A weak hump at 641.6 eV is due to a small amount of MnO_2. The 529.0 eV O 1s peak corresponds to adsorbed oxygen [22], and the weaker, 531.6 eV peak corresponds to MnO_2 [22]. On irradiation, the Bi peak shifts by −1.1 eV to pure Bi value, indicating the phase separation of Bi. A similar but opposite (+1.4 eV) shift in the main Mn peak after irradiation is in accordance with the Bi peak shift [23]. This peak still not occurring at the pure Mn position (638.7 eV) indicates the presence of Mn-rich Mn–Bi phase. The O
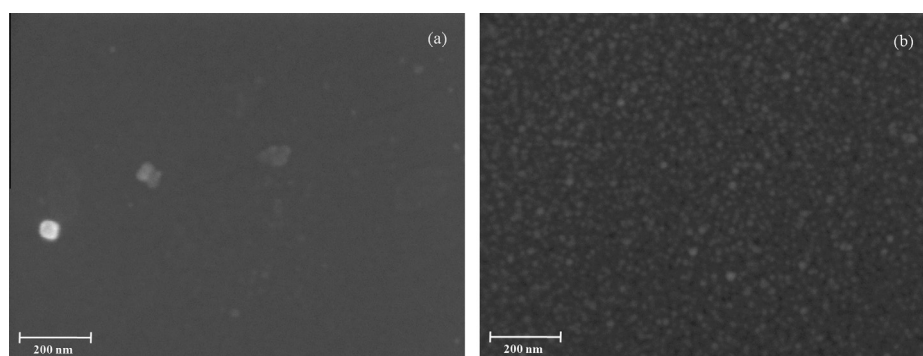

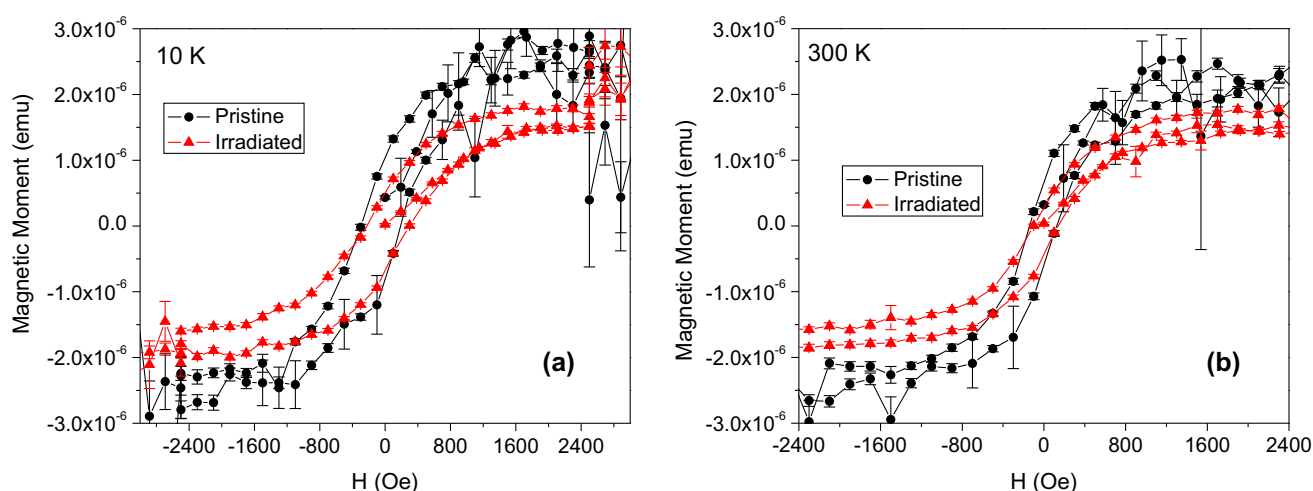Fig. 1. FESEM images of (a) pristine and (b) irradiated samples.

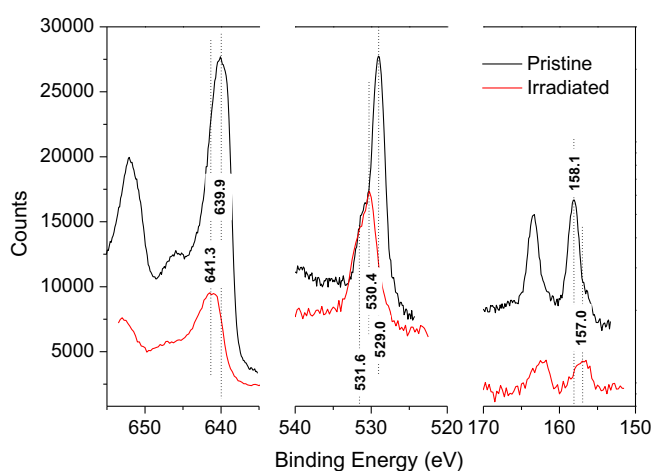**Fig. 3.** Magnetic hysteresis (M–H) curves for pristine and irradiated samples at (a) 10 K and (b) 300 K.

Fig. 4. XPS spectra of pristine and irradiated samples in Bi $4f_{7/2}$, O 1s and Mn $2p_{3/2}$ regions of binding energy.

Fig. 5. Load–displacement curves in various attempts for pristine (dotted lines) and irradiated (solid lines) samples.

1s peaks, occurring at 530.4 eV and 531.6 eV, still correspond to adsorbed oxygen and MnO_2, respectively. Thus, the XPS results suggest a phase separation of Bi and Mn-rich phases on irradiation.

3.5. Nanoindentation

The load–displacement curves for pristine and irradiated samples for a number of measurement attempts are shown in Fig. 5. For the pristine sample, almost the same curves are reproduced in all attempts, indicating this to be a laterally homogeneous film. The mean hardness as derived from hardness versus contact depth curve (not shown) is 10.3 GPa. From the curves after irradiation, two observations can be made. (i) There are many curves in different attempts, indicating lateral inhomogeneity, akin to a structure with soft phases embedded in a hard matrix. (ii) The unloading curves for irradiated samples have smaller slopes than the pristine ones, indicating a softening in the thin film on irradiation [24]. This is corroborated by the 5.6 GPa mean hardness obtained by the hardness versus contact depth measurement.

3.6. Possible mechanism

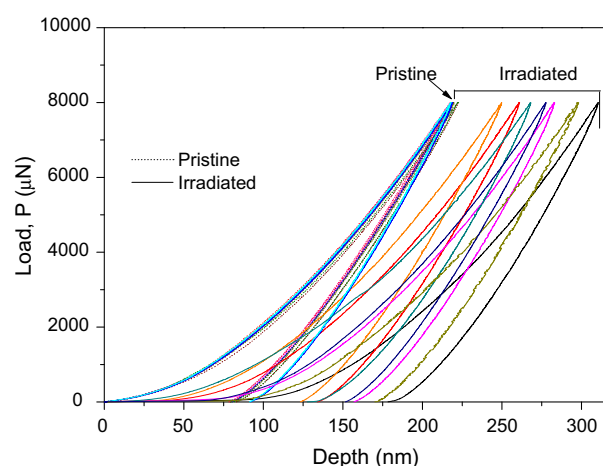The results from the various characterizations discussed above lead to a common conjecture that the SHI irradiation has induced phase separation of Bi and Mn-rich Mn–Bi phases in a homogeneous Mn–Bi composite. Since the S_e is dominant and the system is metallic, the energy transfer mechanism from electronic to lattice subsystem can be assumed to be the e–p coupling [8] as described by the thermal spike model. It is reported earlier [8] that lattice temperatures of Fe can be raised to about 2000 °C in about 3 nm radius cylinder around the 200 MeV Au ion ($S_e \sim 45.8$ keV/nm); it takes about 1×10^{13} ions/cm^2 to fill the whole sample with ion tracks of this diameter. Since the e–p coupling strength (10^3 - W cm^{-3} K^{-1}) in Mn–Bi is about an order of magnitude greater than that for Fe (125 W cm^{-3} K^{-1}), it can be safely assumed (i) that the miscible liquid temperatures (>1800 K) can be easily achieved by the present S_e value, and (ii) that the 1×10^{13} ions/cm^2 fluence is sufficient to fill the whole sample with ion tracks in the present case also. The molten Mn Bi liquid, while passing through the liquid immiscibility region on rapid cooling [15], creates separation of immiscible liquid phases, freezes subsequently, and thus leads to the formation of the observed structure.

4. Conclusion

In the present work, pulsed laser deposited homogeneous $Mn_{0.82}Bi_{0.18}$ thin film was irradiated by 100 MeV Au ions at 1×10^{13} ions/cm^2 fluence. The FESEM pictures reveal the

emergence of ~20 nm diameter nanostructures of Bi-rich phase dispersed in Mn-rich matrix on irradiation. The post-irradiation enhancement in Bi and Mn-rich Mn–Bi XRD peaks and the emergence of a new Mn-rich Mn–Bi peak corroborate the phase separation phenomenon, while XRR of the pristine samples reveals the thickness of the film to be 60 nm. The persistence of magnetic hysteresis loop with reduced area and symmetric Mn and Bi XPS peak shifts also suggest the Mn-rich Mn–Bi phase separation. A reduction in the mean hardness and emergence of lateral inhomogeneity is an evidence of formation of softer phases dispersed in a harder matrix on irradiation. Thus, all the characterization measurements collectively suggest that 100 MeV ion irradiation of a homogeneous mixture of Mn and Bi has led to the synthesis of Bi nanostructures dispersed in Mn-rich Mn–Bi matrix.

Acknowledgements

References

[1] B. Predel et al., in: H.U. Walter, M.F. Ashhy (Eds.), Decomposition of Alloys: The Early Stages, Springer, Berlin, 1987, p. 517.
[2] L. Ratke, S. Diefenbach, Mater. Sci. Eng. 15 (1995) 263.
[3] Y. Yong, X. Li, Trans. ASME 129 (2007) 252.
[4] X. Fang, Z. Fan, Mater. Sci. Technol. 21 (2005) 366.
[5] T. Carlberg, H. Frederiksson, Metall. Trans. A 11A (1980) 1665.
[6] H.C. deGroh III, H.B. Probst, J. Spacecraft Rockets 26 (1989) 476.
[7] Z.G. Wang, Ch. Dufour, E. Paumier, M. Toulemonde, J. Phys. Condens. Matter 6 (1994) 6733.
[8] S.K. Srivastava, D.K. Avasthi, W. Assmann, Z.G. Wang, H. Kucal, E. Jacquet, H.D. Carstanjen, M. Toulemonde, Phys. Rev. B 71 (2005) 193405.
[9] S.K. Srivastava, D.K. Avasthi, E. Pippel, Nanotechnology 17 (2006) 2518.
[10] Amit Kumar et al., Nucl. Instr. Meth. Phys. Res. B 244 (2006) 23.
[11] B.Z. Rameev et al., Microelectronic Eng. 69 (2003) 330.
[12] S.A. Khan, S.K. Srivastava, D.K. Avasthi, J. Phys. D: Appl. Phys. 45 (2012) 375304.
[13] R. Enrique, F. Wu, P. Bellon, Surf. Coat. Technol. 150 (2002) 1.
[14] Y. Gao et al., J. Nucl. Mater. 413 (2011) 11.
[15] T.B. Massalski, Binary Alloy Phase Diagrams, second ed., vol. 1, 1990, A.S.M. International, p. 759.
[16] J.P. Biersack, Nucl. Instr. Meth. Phys. Res. B 27 (1987) 21.
[17] Inorganic Materials Database – AtomWork, <http://crystdb.nims.go.jp/index_en.html>.
[18] Tables de Constantes et Données Numérique, Volume 7, Relaxation Paramagnetique, Masson, Paris, 1957.
[19] W. Hui et al., Trans. Nonferrous Met. Soc. China 13 (2003) 1405.
[20] Yunsheng Dai et al., Catal. Lett. 123 (2008) 307.
[21] M.C. Besinger et al., Appl. Surf. Sci. 257 (2011) 2717.
[22] <www.xpsdata.com/XI_BE_Lookup_table.pdf>.
[23] J.J. Kolodzeij, T.E. Madey, J.W. Keister, J.E. Rowe, Phys. Rev. B 62 (2000) 5150.
[24] M.F. Doerner, W.D. Nix, J. Mater. Res. 1 (1986) 601.